

Three-Dimensional Measurement Using Multiple Slits with a Random Dot Pattern

- Multiple Slits and Camera Calibration -

KUMIKO YOSHIDA^{*1} and KIKUHITO KAWASUE^{*1}

^{*1} Department of Environmental Robotics

University of Miyazaki

1-1 Gakuen Kibandai Nishi, Miyazaki

889-2192, JAPAN

kawasue@cc.miyazaki-u.ac.jp

Abstract: Computer vision systems have been used to detect three-dimensional shape data of objects. Slit-laser sweeping or several pattern projections are generated during the recording process when using these systems. Generally, since the recording process requires time, it is necessary to temporarily stop the movement of both the measurement target and the measurement device during the recording process. In order to address this problem, we have developed a measurement system that projects multiple slits with random dots. Three-dimensional shape data can be detected by a single shot. In the proposed method, each slit must be identified in order to judge the projection direction. Random dots are projected onto the same area of multiple slits, and the pattern of random dots is used to identify the slit. In the present paper, an effective calibration method for the system and a method by which to separate each slit and dot pattern in the image are introduced.

Key-Words: Calibration, Computer vision, Random dots, Point cloud, Multiple slits, Laser, Three-dimensional

1 Introduction

A point cloud is a set of vertices in a three-dimensional (3D) coordinate system[1-4]. Point clouds are used in CAD data and robot vision systems. In recent years, inexpensive devices, such as Microsoft KINECT [5-7], that detect 3D point cloud data have become available. Such devices are useful for capturing motion or modeling systems that do not require high accuracy. Such devices are very attractive because they can obtain thousands of point cloud data sets in real time. However, the data obtained are not sufficiently accurate for industrial applications. Furthermore, for such systems to be used in industrial applications, an easy method of extracting the desired data from the enormous amount of point cloud data is required. The reason for this is that automatic extraction of target objects requires very extensive computer processing because point cloud data include a great deal of redundant data, such as background data.

The slit-ray projection method [8-11] (i.e., shape from structured light) is widely used in industrial applications and robot vision systems. This method has high measurement accuracy. In the slit-ray projection method, a laser slit is projected onto the surface of the target object and the laser streak generated on the surface is detected by a camera. The 3D position data of the laser slit are estimated by triangulating the orientation of the laser projector and

the camera[12]. The process of extracting valuable data from the enormous amount of cloud data obtained is simplified because the slit-ray projection method detects point data from the location at which the laser streak is projected.

In implementing the slit-ray projection method, the laser slit should be swept to cover the entire surface of the object. Therefore, it is necessary to temporarily stop the movement of both the measurement target and the measurement device during the recording process.

Multiple-slit projection methods have been introduced to shorten the recording process[13-14]. In implementing these methods, extraction and identification of the slit or pattern are required. The random cuts method of slit-ray projection was introduced to identify each slit [15]. In this method, each slit is divided into numerous small line segments, and stereo matching is carried out in order to obtain three-dimensional data using these segments as features. However, the cut positions of structured light may generate noise. Since a streak of structured light reflects the shape of the measurement target and is the most important parameter in the measurement, extensive modification of structured light is not desirable. A random cut may be located at the edge of an object, which is an important position for determining the size of the object. Therefore, this causes ambiguities in the size measurement of

objects. Intensity modulation or color-coded methods have also been introduced in order to identify slits [16-19]. However, the intensity or color of light is easily influenced by the surrounding environment and the color of the object itself because the intensity of the structured light cannot be maintained at a high level for modulation purposes.

In order to address this problem, we have developed a measurement system that projects multiple slits with random dots. Three-dimensional shape data can be detected from a single shot. In realizing the proposed method, each slit projection must be identified in order to judge the projection direction. Random dots are projected onto the same area of as the slits, and the pattern of random dots is used to identify the slits. Neither the measurement device nor the measurement object need be stopped during the measurement.

In the present paper, the proposed system is outlined, and the effectiveness of the calibration method is investigated. Moreover, a method of separating each slit and dot pattern from the image and experimental results are introduced.

2 Measurement System

2.1 Slit-ray Projection Method

Fig. 1 shows the principle of the general slit-ray projection method. In this figure, a single slit is projected against the wall from different distances. The slit is displaced depending on the distance from the system. Therefore, the distance between the wall and the system can be measured by examining the displacement of the slit [20].

Fig. 2 shows a schematic diagram of the shape measurement system. Points on the slit can be calculated by triangulation considering the direction of the laser slit. Therefore, the cross sectional shape of the laser slit can be estimated. In order to measure the shape of an entire object, sweeping of the slit is required.

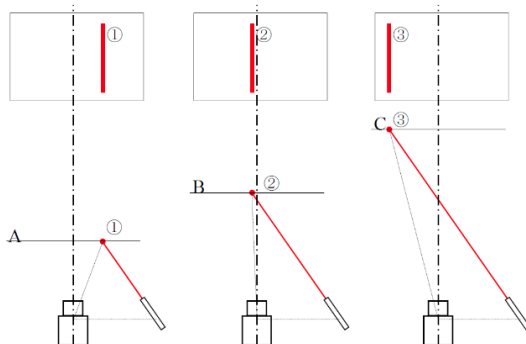


Fig. 1 Laser projection and camera setup

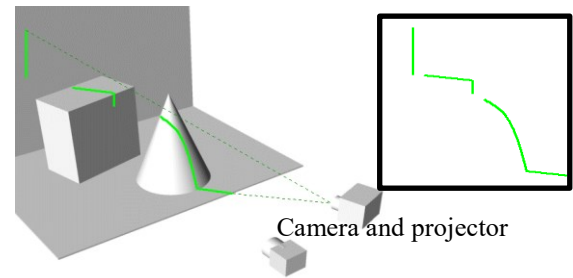


Fig. 2 Shape measurement

2.2 Multiple-Slit Projection Method

Fig. 3 shows a schematic diagram of the multiple slit-ray projection method. Increasing the slit number increases the number of measurement cross-sections. However, each slit has to be distinguished and the direction of the projection should be known for the purpose of triangulation. In the measurement image, a number of line segments that have different laser direction exist, which causes difficulty in automatic image analysis.

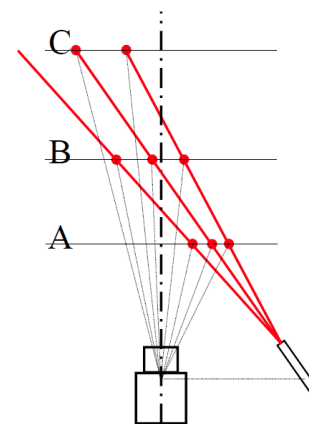
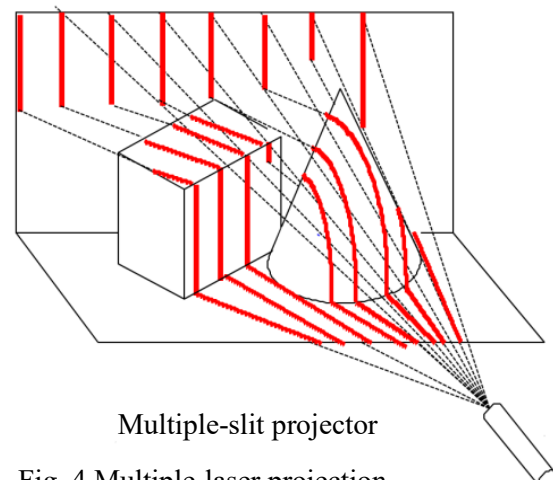


Fig. 3 Schematic diagram of multiple-slit projection



Multiple-slit projector

Fig. 4 Multiple-laser projection

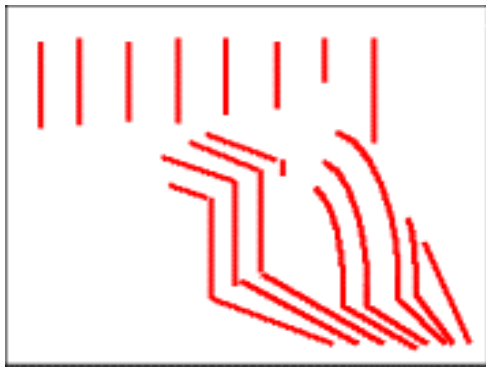


Fig. 5 Recorded image of multiple slits

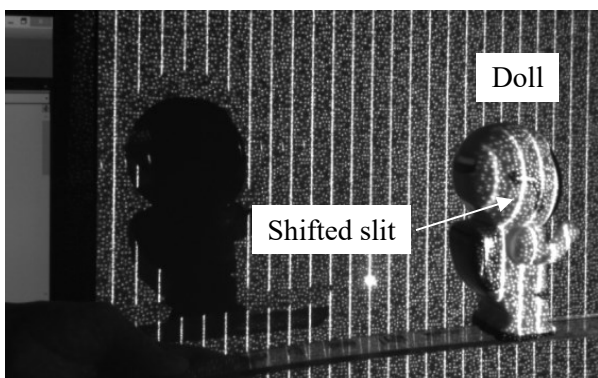


Fig. 6 Captured image

Fig. 4 shows the projection of multiple lasers onto the surface of an object. Figs. 5 and 6 show images recorded by camera. In Fig. 4, the dotted line helps in identifying the direction of the laser slit. Note, however, that recognizing the direction of the laser slit on the actual recorded image, as shown in Figs. 5 and 6, is difficult. In Fig. 6, some laser slits are shifted from the original position by the doll. This shifting causes difficulty in slit identification.

2.3 Multiple Slits with Random Dots

In order to cope with the ambiguity of the recognition of each slit, we propose multiple-laser-slit projection with random dots. Fig. 7 shows a schematic diagram of the system used to project multiple laser slits with random dots onto the surface of the objects. Random dots are simultaneously projected along the laser slit and the random dots enable us to identify each slit. Fig. 8 shows an example image of these random dots. This random-dot pattern is used to identify the slit address number. Multiple slits and random dots are generated by placing a diffraction plate in front of the laser projector.

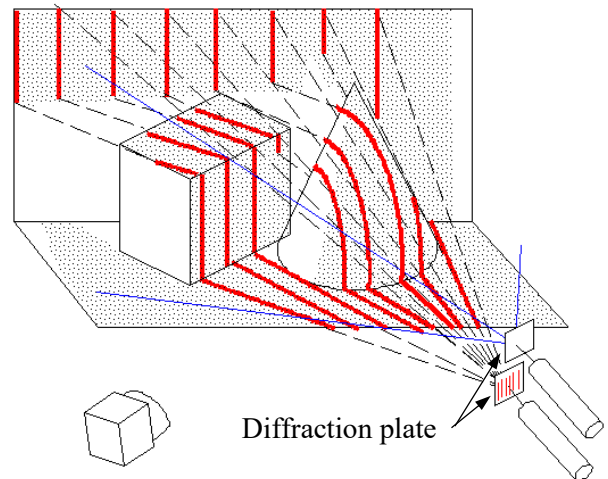


Fig. 7 System setup

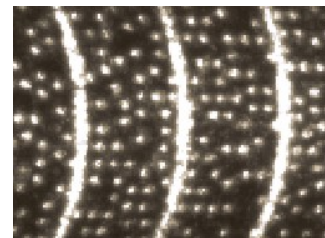
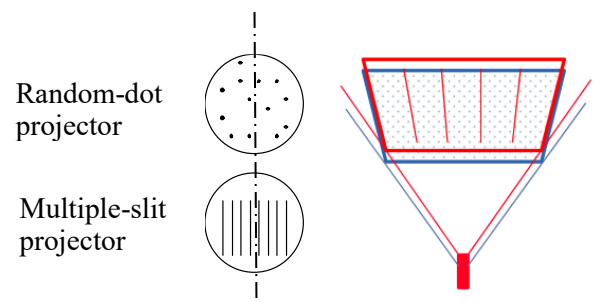
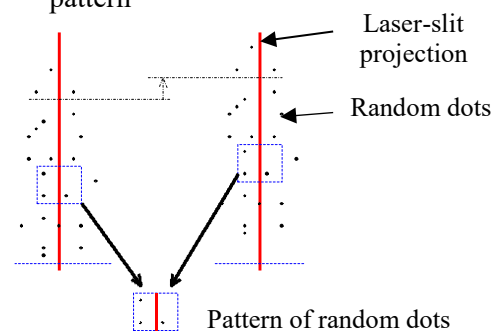


Fig. 8 Random dots projected along the slit



(a) Arrangement of projectors and shifted pattern



(b) Projected pattern

Fig. 9 Shift between laser-slit projection and random-dot pattern

Note that the multiple-slit projector and the random-dot projector are arranged vertically in the system. The difference in position between the multiple-slit projector and the random-dot projector causes a slight displacement (which depends on the distance between the projectors) on the surface of the target, as shown in Fig. 9. However, the assignment results of the slit addresses are not affected, because the displacement occurs along the direction of the slit line. As is shown in this figure, the pattern of random dots is not shifted horizontally with respect to the slit.

3 Measurement Flow

The initial setting is realized before measurement. In the initial setting, a “reference image” indicating the position of the slit with random dots and the slit line number is obtained. The laser slit and random dots are then projected onto a plain board. The projection of the slit and random dots onto the board is then recorded. The distance between the measurement system and the board is then changed, and the procedure is repeated a couple of times. Reference images are recorded during this process. The line equations of the slits are determined for each slit in the reference image. Fig. 10 shows an example of a reference image. 25 slits are captured in this reference image, and we refer to these as “reference lines”. The reference image is used to assign addresses to the slits.

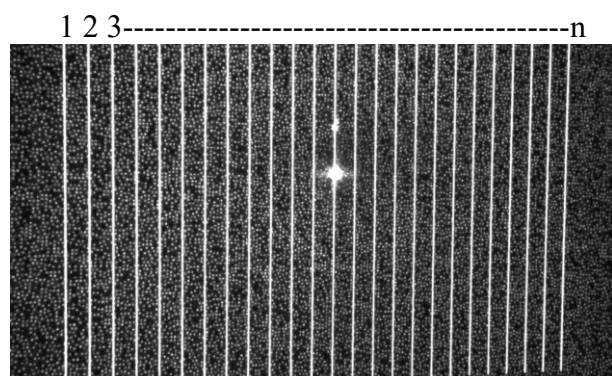


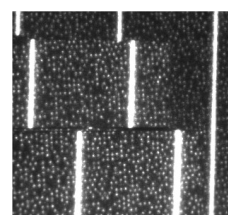
Fig. 10 Reference image

4 Extraction and Identification of Slit Addresses

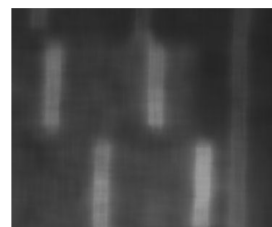
4.1 Extraction of Slits

Fig. 11(a) shows the original image captured by the system. Multiple slits and random dots are recorded simultaneously in an image. First, a median filter is applied to the original image. Image (b) is obtained by applying the median filter. By subtracting image (b) from the original image (a), we obtain image (c),

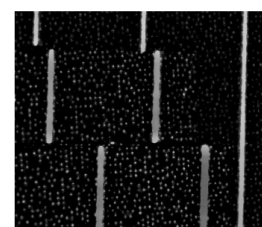
which emphasizes the slits and random dots. The random dots can be deleted by applying morphology processing[21-23]. Generally, morphology processing is applied for noise reduction but can also be used to remove dots, as shown in image (d). Once the slit is extracted properly, the dots can be easily extracted by subtracting image (d) from image (c). The extracted dots are shown in image (e). Two separated images of multiple slits and random dots are used for the line number assignment.



(a) Original image



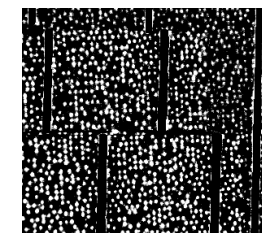
(b) Median filter



(c) Result of subtracting (b) from (a)



(d) Slit extraction by morphology



(e) Dot extraction by subtracting (d) from (c)

Fig. 11 Extraction of slits and random dots

4.2 Identification of Slit Address

Fig. 12 shows the slit address assignment procedure. A number of points (A_j) on the slit are randomly selected and the template area is set around the point. The pattern of random dots is used to identify each slit. The area having the same pattern of dots as the selected template is searched on the reference image using a template matching technique[24-26]. In the search process, Epipolar geometry is used for quick search. Once the arrangement between the laser projectors and the camera is fixed, the epipolar geometry can be determined[27-30]. The search area of the reference image is estimated using the epipolar geometry. The search area is on the straight line, as shown in Fig. 13. Since the slit equations have been determined, the points matching the template are

limited at the intersection points between the slit line equations and the epipolar line. This technique enables fast image processing for the assignment of slit addresses.

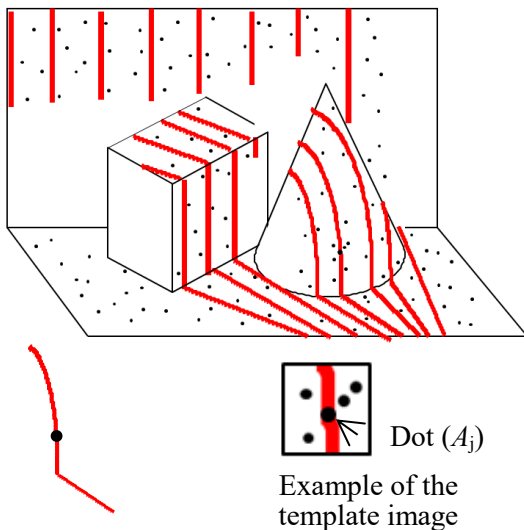


Fig. 12 Template on the slit

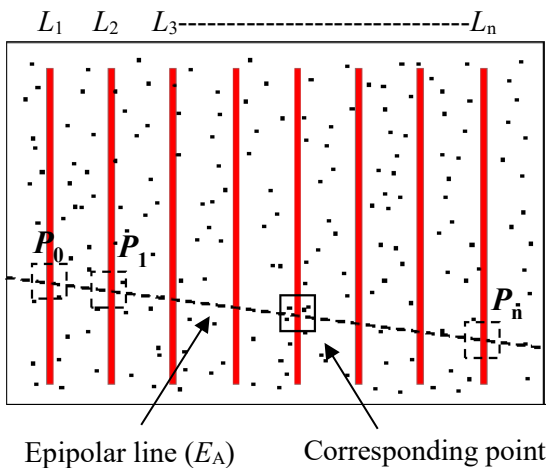


Fig. 13 Assignment of slit addresses on the reference image

5 Calibration of the System and Calculation of Grobal Coordinates

5.1 Coordinate Systems for Measurement

The measurement position of the global coordinate system can be determined uniquely by finding the intersection point between a slit ray and the line-of-sight of the camera. The line-of-sight of the camera passes through the measurement point and the focal point of the camera. Fig. 14 shows the relations between the global coordinate system (X,Y,Z) , the camera coordinate system (u,v) fixed on the camera,

and the projector coordinate system (X_p) fixed on the multiple-slit projector. The camera parameters indicate the relation between the global coordinate system and the camera coordinate system, and the projector parameters indicate the relation between the global coordinate the projector coordinate. The measurement point in global coordinates can be estimated by combining the camera parameters and the projector parameters. The combined parameters are referred to as the system parameters. A flowchart of this procedure is shown in Fig. 15.

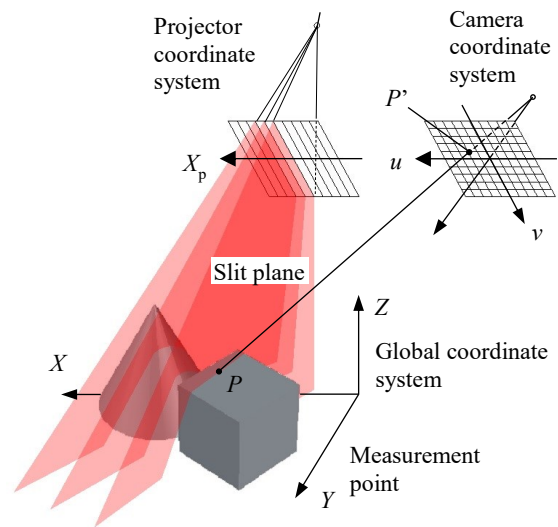


Fig. 14 Relations between coordinate systems

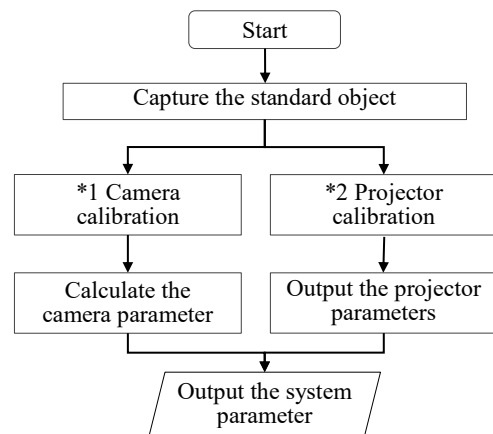


Fig. 15 Flowchart of system calibration

5.2 Camera Parameters

The relation between the global coordinate system (X,Y,Z) and the camera coordinate system (u,v) in terms of homogeneous coordinates is as follows [31]:

$$\begin{bmatrix} H_c u \\ H_c v \\ H_c \end{bmatrix} = \begin{bmatrix} c_{11} & c_{12} & c_{13} & c_{14} \\ c_{21} & c_{22} & c_{23} & c_{24} \\ c_{31} & c_{32} & c_{33} & c_{34} \end{bmatrix} \begin{bmatrix} X \\ Y \\ Z \\ 1 \end{bmatrix} \quad (1)$$

where c_{11} through c_{34} are the camera parameters, and H_c is an extra parameter for homogeneous coordinate systems. Camera parameters include the data such as the position, orientation, and magnification in global coordinates. Eq. (1) is transformed as follows by eliminating H_c :

$$\begin{aligned} (c_{11}-c_{31}u)X+(c_{12}-c_{32}u)Y+(c_{13}-c_{33}u)Z=c_{34}u-c_{14} \\ (c_{21}-c_{31}v)X+(c_{22}-c_{32}v)Y+(c_{23}-c_{33}v)Z=c_{34}v-c_{24} \end{aligned} \quad (2)$$

By feeding the corresponding pairs of data into the global coordinate system (X,Y,Z) and the camera coordinate system (u,v) , the equations given in Eq. (2) are obtained. Since the number of unknown values (c_{11} through c_{34}) of the camera parameters is twelve, the camera parameters can be estimated by feeding six non-coplanar points for which the positions are known into the equations. The intersection of the two planes given by Eq. (2) is the line-of-sight of the camera that passes through the measure point (X,Y,Z) and the image plane at (u,v) .

5.3 Projector Parameters

The relation between the projector coordinate system and the global coordinate system can be expressed in the same manner as the relation between the camera coordinate system and the global coordinate system. Therefore, the following equation is established by replacing the camera coordinate system by the projector coordinate system:

$$\begin{bmatrix} H_p X_p \\ H_p \end{bmatrix} = \begin{bmatrix} P_{11} & P_{12} & P_{13} & P_{14} \\ P_{21} & P_{22} & P_{23} & P_{24} \end{bmatrix} \begin{bmatrix} X \\ Y \\ Z \\ 1 \end{bmatrix} \quad (3)$$

As the slit lines are arranged along one direction, the slit position can be indicated by just one variable (X_p). By eliminating the extra parameter (H_p), the equation is transformed as follows:

$$\begin{aligned} (P_{11}-P_{21}X_p)X+(P_{12}-P_{22}X_p)Y+(P_{13}-P_{23}X_p)Z \\ =P_{24}X_p-P_{14} \end{aligned} \quad (4)$$

This is the equation of the laser plane indicated by slit position X_p . Since the number of unknown values (P_{11} through P_{24}) is eight, these unknown values can be estimated by feeding eight

corresponding data (X_p) for which the positions (X,Y,Z) are known.

5.4 Data Sets for Calibrations

Both the camera parameters and the projector parameter are estimated using sets of corresponding points in different coordinate systems. The positions of these point sets should be known. Fig. 16 shows the standard object to which checkerboard markers and a scale are affixed. The global coordinate system is fixed to the standard object. Checkerboard markers and a scale are affixed to the frame of the standard object. A magnified image of the frame is shown in the figure. The checkerboard makers are

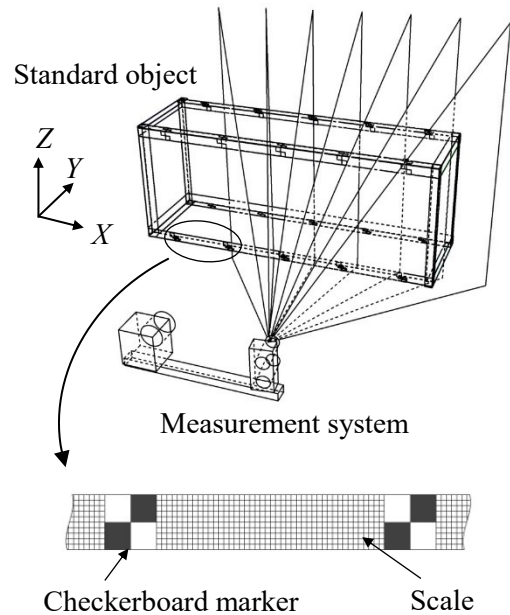


Fig. 16 Calibration setup

*1 Camera calibration

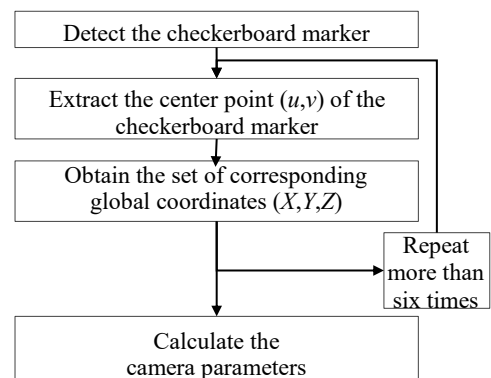


Fig. 17 Flowchart of camera calibration

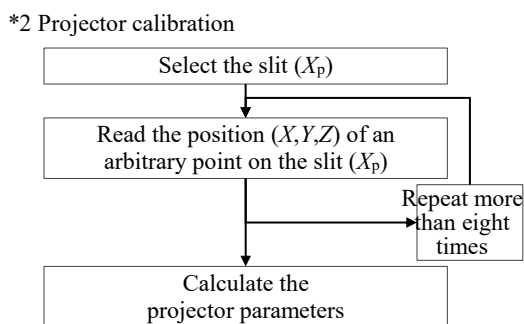


Fig. 18 Flowchart of projector calibration

used for camera calibration, and the scales are used for projector calibration. Figs. 17 and 18 are flowcharts of the camera calibration and projector calibration procedures, respectively. In order to improve the precision of the calibration, a number of corresponding points should be fed into the equations, and the final parameters are determined by the least-squares method.

5.5 System Parameters and Conversion to the Global Coordinate System

Camera parameter C indicates the line-of-sight of the camera that passes through the measurement point and the focal point of the camera, and projector parameter P indicates the slit plane with the slit number. Therefore, the measurement position can be estimated by calculating the cross point between the line-of-sight of the camera and the slit plane. A flowchart of the procedure is shown in Fig. 19. The point (u,v) on slit X_p in the image is converted to global coordinates by Eqs. (1) and (3). The combined parameters are referred to collectively as the system parameters.

These equations are arranged as follows:

$$F=QV \tag{5}$$

where

$$F = \begin{bmatrix} c_{34}u - c_{14} \\ c_{34}v - c_{24} \\ P_{24}X_p - P_{14} \end{bmatrix}$$

$$Q = \begin{bmatrix} c_{11} - c_{31}u & c_{12} - c_{32}u & c_{13} - c_{33}u \\ c_{21} - c_{31}v & c_{22} - c_{32}v & c_{23} - c_{33}v \\ P_{11} - P_{21}X_p & P_{12} - P_{22}X_p & P_{13} - P_{23}X_p \end{bmatrix}$$

$$V = \begin{bmatrix} X \\ Y \\ Z \end{bmatrix} \tag{6}$$

Therefore,

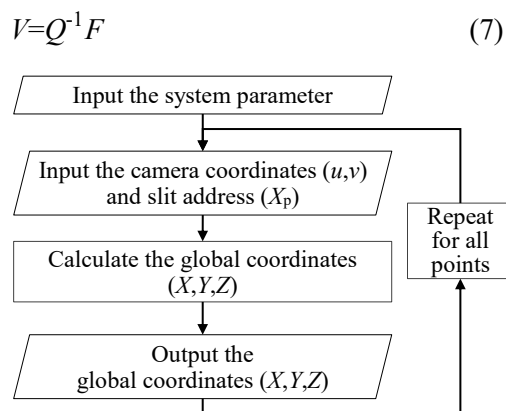


Fig. 19 Flowchart of conversion to global coordinates

6 Experiment

Fig. 20 shows a photograph of the measurement system. A multiple-laser-slit projector (20 mW) and a random-dot projector (30 mW) are arranged vertically on one side of the rod, and the camera (Basler acA1300 60 fps) is placed at the other side of the rod while maintaining a constant baseline length (450 mm) with respect to the laser projector.

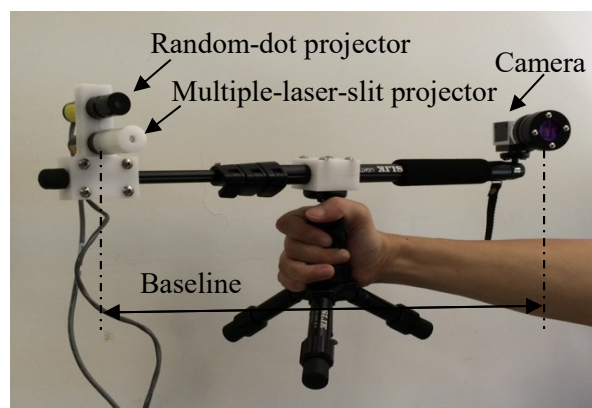


Fig. 20 Multiple-laser projector and random-dot projector system and camera

6.1 Slit Address Assignment

Fig. 21 shows the object used in the experiment. Seven slits with random dots are projected onto the surface of the object. Fig. 22 shows the recorded image and one example of the template. Fig. 23 shows the results of assigning the slit addresses, and the encircled slit was assigned an incorrect address. However, most of the slits were assigned the correct address. Fig. 24 shows the measurement points displayed on computer.

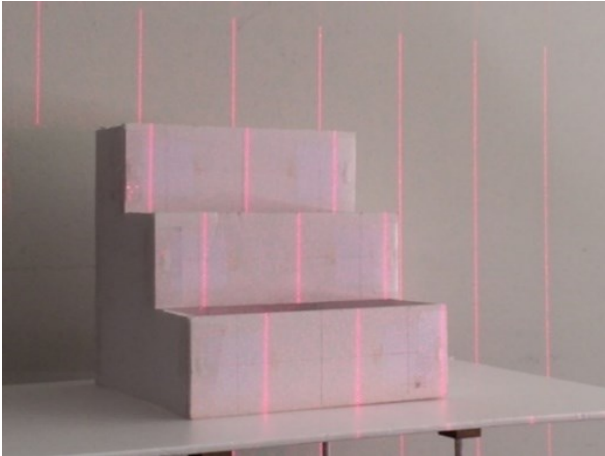


Fig. 21 Measurement object

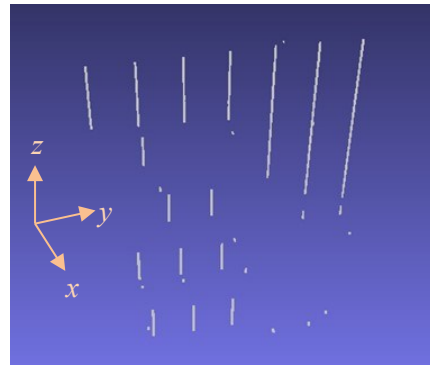


Fig. 24 Calculated points in the global coordinate system

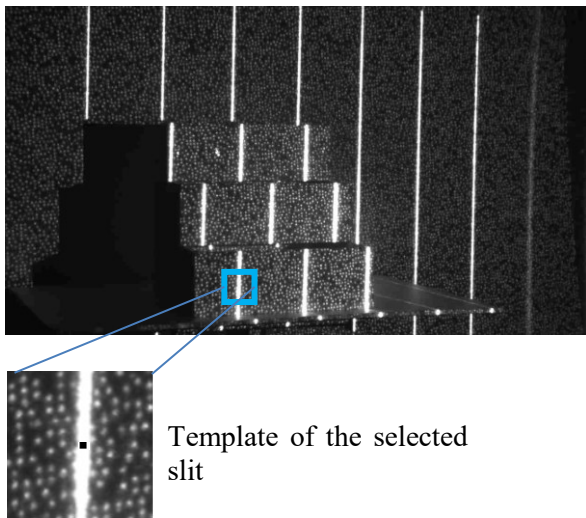


Fig. 22 Image recorded by the camera

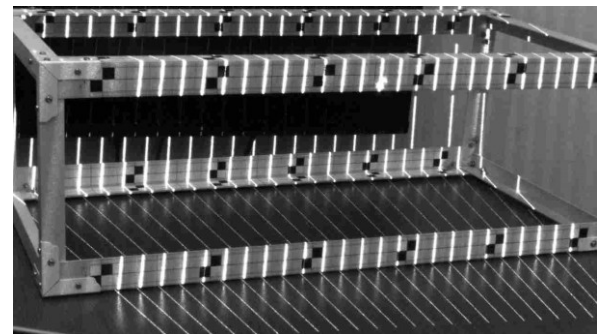


Fig. 25 Standard object

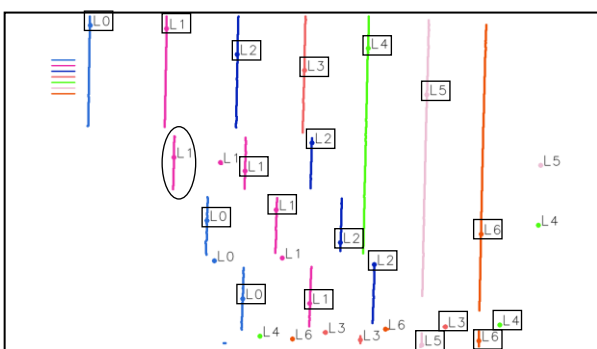


Fig. 23 Final assignment of slit addresses

6.2 Calibration and Measurement

Simple experiments were conducted in order to evaluate the estimation performance of the global coordinates of the measurement point.

A photograph of the standard object used in the calibration is shown in Fig. 25. The standard object is 200 mm × 300 mm × 500 mm and is set at a distance of approximately 1,000 mm from the measurement system.

6.2.1 Camera Calibration

The positions of the measurement system and standard object are fixed, and the image of the standard object is captured. The position of the checkerboard marker is used for to obtain the camera parameters and is known in the global coordinates. The checkerboard marker is detected in the captured image, and the position of the center corner (u_i, v_i), as indicated by the colored point in Fig. 26, in the checkerboard marker is automatically extracted by the computer. By repeating this procedure at least six times, corresponding position data between the global coordinate system and the camera coordinate system are fed into the computer, and the camera parameters are determined. Over eight points were selected in our experiments. Note that the selected checkerboard markers are not coplanar in the global coordinate system.

6.2.2 Projector Calibration

The positions of the measurement system and standard object are fixed, and multiple slits are projected onto the standard object.

Fig. 27 shows the scale attached to frame of the standard object. Red lines are multiple slits projected onto the standard object. A number of points are selected on the slit, the global positions of which are read manually. The global coordinates of the selected positions on the slits and the slit number are fed to the computer, and the projector parameters are determined. Over 12 points were selected in these experiments.

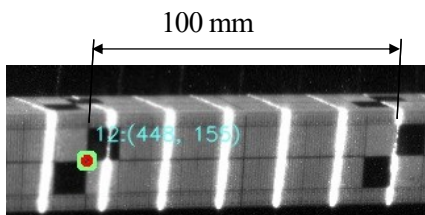


Fig. 26 Checkerboard markers used in camera calibration

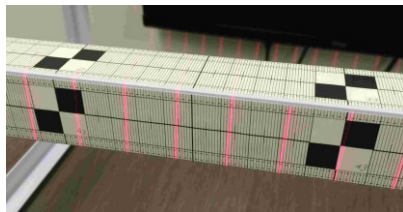
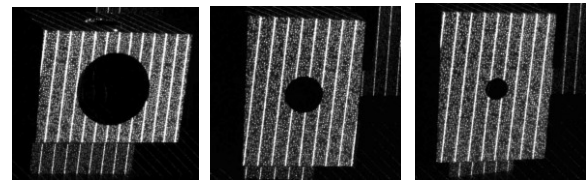


Fig. 27 Scale used in projector calibration

6.2.3 Measurement Performance

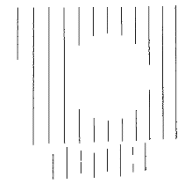
A flat board with a hole was used as the measurement object. Multiple slits were projected around the hole, and the detected edge positions were used for measurement evaluation. The diameters of the holes were 100 mm, 50 mm, and 30 mm, and the distance from the system was approximately 0.9 m. Fig. 28(a) shows the captured image, and Fig. 28(b) shows the detected data for the hole (size = 100 mm) in global coordinates.

Fig. 28(c) shows the detected edges. The diameter of the hole was estimated based on the positions of the edges detected using circle estimation. Table 1 shows the results of the hole measurement. The measurement error was less than 0.5 mm.



D1 (φ 100 mm) D2 (φ 50 mm) D3 (φ 30 mm)

(a) Recorded image



(b) Three-dimensional shape of the object (D1)



(c) Detected edge of the hole

Fig. 28 Detection of the edge of the hole and hole size measurement

Table 1 Results of the estimation of the hole diameter

	Actual diameter [mm]	Estimated diameter [mm]	Error [mm]
D1	100.0	99.7	-0.3
D2	50.0	49.5	-0.5
D3	30.0	29.9	-0.1

7 Conclusions

We proposed a three-dimensional measurement system using multiple laser projection with random dots. Three-dimensional shape data can be detected from a single image. In realizing the proposed method, random dots are projected onto the same area as multiple slits. The pattern of random dots is used to identify the slits. The proposed method enables the effective assignment of slit addresses. Neither the measurement device nor the measurement object needs to be stopped during measurement.

The results of the proposed paper are summarized as follows.

- (1) A multiple-slit projection method with random dots was introduced.
- (2) The system calibration and calculation method of the measured points in global coordinates was described.
- (3) The extraction method of multiple slits and random dots from the captured image was introduced.

- (4) An effective calibration method using a standard object with checkerboard markers and a scale was introduced.
- (5) The detected measurement points in global coordinates were displayed on a computer, and the feasibility of the proposed system was demonstrated.
- (6) The measurement results for the dimensions of a hole in a plate were presented.

References:

- [1] Pottmann, H., Leopoldseider, S., Hofer, M.: Registration without icp. *Computer Vision and Image Understanding* 95(1) (July 2004) 54-71
- [2] Pottmann, H., Hofer, M., Odehnal, B., Wallner, J.: Line geometry for 3d shape understanding and reconstruction. In: *Proc. ECCV04. (2004) Vol I: 297-309*
- [3] Hofer, M., Odehnal, B., Pottmann, H., Steiner, T., Wallner, J.: 3d shape recognition and reconstruction based on line element geometry. In: *Proc. ICCV05. (2005)II: 1532-1538*
- [4] Pottmann, H., Huang, Q., Yang, Y., Hu, S.: Geometry and convergence analysis of algorithms for registration of 3d shapes. *IJCV* 67(3) (May 2006) 277-296
- [5] A. Bigdelou, T. Benz, L.Schwarz, N. Navab, Simultaneous categorical and spatio-temporal 3d gestures using kinect. *Proc. of 2013 IEEE Symposium on 3D User Interfaces*, 2012, pp.53-60.
- [6] C. Dal Mutto, P. Zanuttigh, G. Cortelazzo, Time-of-Flight Cameras and Microsoft Kinect., *Springer Briefs in Electrical and Computer Engineering*, 2012
- [7] Z. Zhang, Microsoft kinect sensor and its effect. *IEEE Multimedia*, Vol.19 , 2012, pp.4-10.
- [8] D. Bhatnagar, A. Pujari, P. Seetharamulu, Static scene analysis using structured light., *Image and Vision Computing*, Vol.9 , 1991, pp.82-87.
- [9] P. Garbat, W. Skarbek, M. Tomaszewski, Structured light camera calibration, *Opto-Electron*, Review 21(1), 2013, pp.23-38.
- [10] Axelsson, L., Karlsson, N.: Object recognition using a laser scanner and fourier-transform. *OptEng* 36(6) (June 1997) 1721-1726
- [11] Guisser, L., Payrissat, R., Castan, S.: A new 3-d surface measurement system using a structured light. In: *CVPR92. (1992) 784-786*
- [12] Funatomi, T., Iiyama, M., Kakusho, K., Minoh, M.: Light stripe triangulation for multiple of moving rigid objects. In: *3DIM07. (2007) 133-140*
- [13] Maki, A.: Geotensity constraint for 3d surface reconstruction under multiple light sources. In: *ECCV00. (2000) I: 725-741*
- [14] Zhang, Y., Yang, Y.: Multiple illuminant direction detection with application to image synthesis. *PAMI* 23(8) (August 2001) 915-920
- [15] M. Maruyama, and S. Abe, Range Sensing by Projecting Multiple Slits with Random Cuts, *IEEE Transactions on Patten Analysis and Machine Intelligence*, Vol.15, No. 6, 1993, pp.647-651.
- [16] Z. J. Geng, Rainbow three-dimensional camera: new concept of high-speed three-dimensional vision systems, *Optical Engineering*, Vol.35, No. 2 ,1996, pp.376-383.
- [17] Li, R., Zha, H.: One-shot scanning using a color stripe pattern. In: *ICPR10. (2010) 1666-1669*
- [18] Lee, K., Je, C., Lee, S.: Color-stripe structured light robust to surface color and discontinuity. In: *ACCV07. (2007) II: 507-516*
- [19] Je, C., Lee, S., Park, R.: High-contrast color-stripe pattern for rapid structured-light range imaging. In: *ECCV04. (2004) Vol I: 95-107*
- [20] Li, Q., Li, F., Shi, G., Qi, F., Shi, Y., Gao, S.: Dense depth acquisition via one-shot stripe structured light. In: *VCIP13. (2013) 1-6*
- [21] Heijmans, H.: Discretization of morphological operators. *JVCIR* 3 (1992) 182-193
- [22] Heijmans, H.: Connected morphological operators for binary images. *CVIU* 73(1)(January 1999) 99-120
- [23] Schonfeld, D.: Optimal nonlinear pattern restoration from noisy binary In: *CVPR92. (1992) 579-584*
- [24] G. Kertész, S. Szénási, Z. Vámosy, Parallelization Methods of the Template Matching Method on Graphics Accelerators, *proc. of 16th IEEE International Symposium on Computational Intelligence and Informatics*, 2015, pp.161-164.
- [25] Nagel, R., Rosenfeld, A.: Ordered search techniques in template matching. *PIEEE* 60(2) (February 1972) 242-244
- [26] Fang, Z., Li, X., Ni, L.: Parallel algorithms for image template matching on hy-percube simd computers. *PAMI* 9(6) (November 1987) 835-841
- [27] Xu, G.: A unified approach to image matching and segmentation in stereo, motion, and object recognition via recovery of epipolar geometry. *Videre* 1(1) (1997) 22-55
- [28] Zhang, Z.: Determining the epipolar geometry and its uncertainty: A review. *IJCV* 27(2) (March 1998) 161-195

- [29] Chai, J., Ma, S.: Robust epipolar geometry estimation using genetic algorithm. PRL 19(9) (July 1998) 829-838
- [30] Boufama, B., Mohr, R.: Epipole and fundamental matrix estimation using virtual parallax. In: ICCV95. (1995) 1030-1036
- [31] C. Torras, Computer Vision: Theory and Industrial Applications, Springer-Verlag, 1992.